acta physica slovaca vol. 45 No. 6, 693 – 704 December 1995

SEMI-CLASSICAL DISTORTED WAVE MODEL FOR MULTI-STEP DIRECT PROCESS IN $(p,p'x)$ AND (p,nx) REACTIONS[1]

M. Kawai
Department of Physics, Kyushu University, Fukuoka 812, Japan

Y. Watanabe[2] and H. Shinohara[3]
Department of Energy Conversion Engineering, Kyushu University, Kasuga, Fukuoka 816, Japan

Received 23 October 1995, accepted 27 October 1995

Present status of Semi-Classical Distorted Wave model (SCDW) for multistep direct (MSD) processes in $(p,p'x)$ and (p,nx) at intermediate energies is discussed. A brief derivation of the cross section formulae for 1-step and 2-step processes is given and their salient features are discussed. Calculated double differential cross sections for ^{60}Ni$(p,p'x)$ at 120 MeV and 200 MeV and for ^{90}Zr(p,nx) at 120 MeV are presented and compared with experimental data. Comparison with other models of MSD is also discussed.

1. Introduction

Understanding the mechanism of pre-equilibrium processes in nuclear reactions has been a subject of extensive studies in recent years. Analyses have been made by means of various models [1]: classical models including several versions of Exciton model and intra-nuclear cascade model (INC), and the quantum mechanical statistical models. Simulations have also been made of late by means of Quantum Molecular Dynamics (QMD) [2] and Antisymmetrized Molecular Dynamics [3].The mechanism seems to be rather complex in general.

In $(p,p'x)$ and (p,n) at intermediate energies, however, the mechanism of emission of high energy nucleons at forward angles seems to be mainly direct processes with relatively small number of steps. Quantum mechanical models of multistep direct process [4] have been proposed and applied to analyses of experimental data. These models are all based on DWBA series expansion of the T-matrix. They differ in statistical

[1] Presented at the International Symposium on Pre-Equilibrium Reactions, Smolenice Castle, – 27 October, 1995

[2] E-mail address: WATANABE@ENCE.KYUSHU-U.AC.JP
[3] Present address: Hitachi Works, Hitachi, Ltd., Japan

assumptions [5] and assumptions on nuclear wave functions and the Green function for propagation of the fast particle in the intermediate states, etc. Simplifying assumptions are also made in practice on form factors of transitions, nuclear state densities etc., which contain some free adjustable parameters.

As an alternative approach, we have proposed a semi-classical distorted wave model (SCDW) [6, 7] which is also based on DWBA expansion. It, however, is greatly simplified by the assumption of the local density Fermi gas model for nuclear states, a local semi-classical approximation to the distorted waves, and Eikonal approximation to the intermediate state Green functions. These approximations are based on the observation that the spatial variation of the local Fermi momentum and of the distorting potentials are small compared with the oscillation of the distorted waves. Under these assumptions, the cross section of each step of MSD processes can be expressed in a simple closed form in terms of the distorting potentials, the nucleon-nucleon scattering cross sections in the nuclear medium, and the nucleon density distribution. These quantities are given either empirically or theoretically, and no free adjustable parameter is involved. The expressions for the cross sections allow simple intuitive interpretation which gives a justification for a basic assumption of INC.

We briefly describe the model and discuss some of its salient features in section 2. In section 3, we present our recent SCDW calculations of the cross sections of 1- and 2-step processes in ^{60}Ni$(p,p'x)$ at 120 MeV and 200 MeV and in ^{90}Zr(p,nx) at 120 MeV and compare with experimental data. We also discuss comparison with previous quantal models and with AMD. A summary and a discussion of future prospect of the model is given in section 4.

2. The model

We start from the DWBA expression

$$\left(\frac{\partial^2\sigma^{(1)}}{\partial E_f \partial\Omega_f}\right) = \frac{1}{2}\sum_{s_i,s_f}\frac{\mu^2}{(2\pi\hbar^2)^2}\frac{k_f}{k_i}\sum_n\left|\left\langle\chi_f^{(-)}\Phi_n\right|\sum_j v_{0j}\left|\chi_i^{(+)}\Phi_0\right\rangle\right|^2\delta(\varepsilon_n-\varepsilon_0-\omega) \quad (1)$$

for the 1-step direct process in A$(p,p'x)$A* where A* is in the continuum. In (1), μ is the reduced mass, $\chi_i^{(+)}(\chi_f^{(-)})$ is the distorted wave in the initial (final) channel at energy $E_i(E_f)$, with the wave number $k_i(k_f)$ and the spin component $s_i(s_f)$ at infinity, $\Phi_0(\Phi_n)$ is the initial (final) state wave function of the nucleus at energy $\varepsilon_0(\varepsilon_n)$, and $\omega = E_i - E_f$ is the energy transfer. The summation extends over all the states n. v_{0j} is the interaction potential between the incident nucleon, 0, and the j-th target nucleon. For simplicity, we assume for the moment that v_{0j} is a central Wigner force, $v_{0j} = v(\mathbf{r}_0 - \mathbf{r}_j)$. This assumption is not made in the actual numerical calculations described later.

We assume single particle model for Φ_0 and Φ_n

$$\Phi_0 = \prod_j \phi_{\alpha_j}, \qquad \Phi_n = \prod_j \phi_{\beta_j} \quad (2)$$

with the single particle wave functions ϕ. All the α are below the Fermi level. Φ_n is a one-particle-one-hole (1p1h) state with a particle in a state β above the Fermi level and a hole in a state α. Thus, one of the $\beta_j = \beta$ is above the Fermi level and one of the $\alpha_j = \alpha$ is missing among the β_j. In coordinate representation, (1) then reads

$$\left(\frac{\partial^2\sigma^{(1)}}{\partial E_f\partial\Omega_f}\right) = C\frac{k_f}{k_i}\sum_{\alpha\beta}\left|\int d\mathbf{r}_0 d\mathbf{r}\chi_f^{(-)*}(\mathbf{r}_0)\phi_\beta^*(\mathbf{r})v(\mathbf{r}_0-\mathbf{r})\chi_i^{(+)}(\mathbf{r}_0)\phi_\alpha(\mathbf{r})\right|^2\delta(\varepsilon_\beta-\varepsilon_\alpha-\omega) \quad (3)$$

where $C = \mu^2/(2\pi\hbar^2)^2$ and $\varepsilon_\alpha(\varepsilon_\beta)$ is the energy of the state $\alpha(\beta)$. On expanding the squared modulus in (3), one has

$$\left(\frac{\partial^2\sigma^{(1)}}{\partial E_f\partial\Omega_f}\right) = C\frac{k_f}{k_i}\sum_{\beta\alpha}\int d\mathbf{r}_0 d\mathbf{r} d\mathbf{r}_0' d\mathbf{r}'\chi_f^{(-)*}(\mathbf{r}_0)v(\mathbf{r}_0-\mathbf{r})\chi_i^{(+)}(\mathbf{r}_0) \times K(\mathbf{r},\mathbf{r}')\chi_f^{(-)}(\mathbf{r}_0')v(\mathbf{r}_0'-\mathbf{r}')\chi_i^{(+)*}(\mathbf{r}_0'), \quad (4)$$

where the kernel $K(\mathbf{r},\mathbf{r}')$ is given by

$$K(\mathbf{r},\mathbf{r}') = \sum_{\beta\alpha}\phi_\beta(\mathbf{r})^*\phi_\alpha(\mathbf{r})\phi_\beta(\mathbf{r}')\phi_\alpha^*(\mathbf{r}')\delta(\varepsilon_\beta-\varepsilon_\alpha-\omega). \quad (5)$$

and is proportional to the imaginary part of the one-particle one-hole Green function. Because of the random phases of the Φ_n, i.e. of the $\phi_\beta(\mathbf{r})^*\phi_\alpha(\mathbf{r})$ and $\phi_\beta(\mathbf{r}')\phi_\alpha^*(\mathbf{r}')$, $K(\mathbf{r},\mathbf{r}')$ is small unless $\mathbf{r}\approx\mathbf{r}'$, in which case the products of the four ϕ are nearly $|\phi_\alpha(\mathbf{r})|^2|\phi_\beta(\mathbf{r})|^2$, and so positive definite. We assume a local density Fermi gas model for the r.h.s of (5) to get

$$K(\mathbf{r},\mathbf{r}') = \frac{1}{(2\pi)^6}\int_{k_\alpha<k_F(\bar{\mathbf{r}}),k_\beta>k_F(\bar{\mathbf{r}})} d\mathbf{k}_\alpha d\mathbf{k}_\beta e^{i(\mathbf{k}_\alpha-\mathbf{k}_\beta)\cdot(\mathbf{r}-\mathbf{r}')}\delta\left(\frac{\hbar^2}{2\mu}(k_\beta^2-k_\alpha^2)-\omega\right), \quad (6)$$

where $k_F(\bar{\mathbf{r}})$ is the Fermi momentum at $\bar{\mathbf{r}} = (\mathbf{r}+\mathbf{r}')/2$. The r.h.s. of (6) is indeed a short ranged function of $s = |\mathbf{r}'-\mathbf{r}|$, peaked at $s=0$. The width of the peak at half maximum turns out to be less than 2 fm even for E_F as low as 1.6 MeV [6], which is much smaller than the nuclear diameter and is of the order of the wave lengths of a distorted wave at 200 MeV.

Since the range of v is also short, the factor

$$v(\mathbf{r}_0-\mathbf{r})K(\mathbf{r},\mathbf{r}')v(\mathbf{r}_0'-\mathbf{r}')$$

in the integrand of (2.4) is only appreciable when $\mathbf{r}_0\approx\mathbf{r}_0'$. If the distorting potential $U_c(\mathbf{r}_0')$ varies slowly with $\mathbf{r}_0'$, a local semi-classical approximation

$$\chi_c(\mathbf{r}_0') \approx \chi_c(\mathbf{r}_0)e^{i\mathbf{k}_c(\mathbf{r}_0)\cdot(\mathbf{r}_0'-\mathbf{r}_0)}, \qquad (c=i,f) \quad (7)$$

will be valid for $\mathbf{r}_0'$ within a small cell, $|\mathbf{r}_0' - \mathbf{r}_0| < d$ with a small distance, d, where $\mathbf{k}_c(\mathbf{r}_0) = -i\nabla\chi_c(\mathbf{r}_0)/\chi_c(\mathbf{r}_0)$ is the local wave number vector with $k_c(\mathbf{r}_0) = [2\mu/\hbar^2(E_c - U_c(\mathbf{r}_0))]^{1/2}$. If, as we assume, the imaginary part of U_c is not too large, we can neglect the variation of the amplitude of $\chi(\mathbf{r}_0')$ within the cell, and assume $\mathbf{k}_c(\mathbf{r}_0)$ to be real in good approximation. In that case, $\mathbf{k}_c(\mathbf{r}_0) \approx \mathrm{Flux}[\chi_c(\mathbf{r}_0)]/|\chi_c(\mathbf{r}_0)|^2$ and $k_c(\mathbf{r}_0) \approx \Re[\{2\mu/\hbar^2(E_c - U_c(\mathbf{r}_0))^{1/2}\}]$.

Putting (6) and (7) into (4), one obtains

$$\left(\frac{\partial^2\sigma^{(1)}}{\partial E_f \partial\Omega_f}\right) = \frac{k_f}{k_i}\left(\frac{A}{A+1}\right)^2 \int \mathrm{d}\mathbf{r} \left|\chi_i^{(+)}(\mathbf{r})\right|^2 \left|\chi_f^{(-)}(\mathbf{r})\right|^2 \frac{k_f/k_f(\mathbf{r})}{k_i/k_i(\mathbf{r})} \left(\frac{\partial^2\sigma}{\partial E_f(\mathbf{r})\partial\Omega_f(\mathbf{r})}\right)_{\mathbf{r}} \rho(\mathbf{r}), \quad (8)$$

where

$$\left(\frac{\partial^2\sigma}{\partial E_f(\mathbf{r})\partial\Omega_f(\mathbf{r})}\right)_{\mathbf{r}} = \frac{4m k_f(\mathbf{r})}{\hbar^2 k_i(\mathbf{r})(4\pi/3)k_F(\mathbf{r})^3} \int_{k<k_F(\mathbf{r})} \mathrm{d}\mathbf{k} \left(\frac{\partial\sigma}{\partial\Omega_\kappa}\right)_{NN} \delta(\kappa'^2 - \kappa^2) \quad (9)$$

is the local average differential cross section of NN scattering where $\boldsymbol{\kappa} = (\mathbf{k}_i(\mathbf{r}) - \mathbf{k})/2$ ($\boldsymbol{\kappa}' = (\mathbf{k}_f(\mathbf{r}) - \mathbf{k}')/2$) is the relative momentum in the 2-nucleon c.m. system where $\mathbf{k}(\mathbf{k}')$ is the momentum of the struck target nucleon in the initial (final) state. The local average cross section, however, is put to 0 if the Pauli principle, $k_f(\mathbf{r}_0), k' > k_F(\mathbf{r}_0)$, is violated. The local kinetic energy, $E_f(\mathbf{r}) = \hbar^2 k_f(\mathbf{r}_0)^2/\mu$, and direction, $\Omega_f(\mathbf{r}) = \hat{\mathbf{k}}_f(\mathbf{r}_0)$, of emission correspond, respectively, to E_f and Ω_f at infinity. In (9),

$$\left(\frac{\partial\sigma}{\partial\Omega_{\kappa'}}\right)_{NN} = \frac{(m/2)^2}{(2\pi\hbar^2)^2}\left|\int \mathrm{d}\mathbf{x} v(\mathbf{x}) e^{-i\mathbf{q}\cdot\mathbf{x}}\right|^2 \quad (10)$$

is the NN scattering cross section with the momentum transfer $\mathbf{q} = \boldsymbol{\kappa}' - \boldsymbol{\kappa} = \mathbf{k}_f(\mathbf{r}_0) - \mathbf{k}_i(\mathbf{r}_0)$. Eq. (8) is the final form of the SCDW cross section for a 1-step process.

The approximations described above can also be used to calculate cross sections of 2-step processes. In the present picture, a 2-step process in $(p, p'x)$ is a successive excitation of two target nucleons, $\alpha_1 \to \beta_1$ and $\alpha_2 \to \beta_2$, except for the rare cases of $\beta_1 \to \beta_2$ and $\alpha_1^{-1} \to \alpha_2^{-1}$ which we neglect. Its T-matrix element is

$$T_{fi}^{(2)} = \sum_{\alpha_1\alpha_2\beta_1\beta_2} \langle \chi_f^{(-)}\phi_{\beta_2}|V|\phi_{\alpha_2}\rangle \frac{1}{E_m - K - U_m + i\eta} \langle \phi_{\beta_1}|V|\chi_i^{(+)}\phi_{\alpha_1}\rangle \quad (11)$$

where $(E_m - K - U_m + i\eta)^{-1}$ is the Green function of relative motion between the fast particle and the nucleus in the intermediate state at energy $E_m = E - (\varepsilon_{\beta_1} - \varepsilon_{\alpha_1})$, with kinetic energy K and distorting potential U_m.

In addition to the same approximations as for the 1-step process, we assume Eikonal approximation to the coordinate representation of the Green function

$$\langle \mathbf{r}_2 \left| \frac{1}{E_m - K - U_m + i\eta} \right| \mathbf{r}_1 \rangle \approx -\frac{2\mu}{\hbar^2} \frac{\exp(ik_m|\mathbf{r}_2 - \mathbf{r}_1|)}{|\mathbf{r}_2 - \mathbf{r}_1|}, \quad (12)$$

where $\mathbf{r}_1(\mathbf{r}_2)$ is the first (second) collision point, and $k_m = [(2\mu\hbar^2)^2(E_m - U_m)]^{1/2} = \kappa_m + i\gamma_m$ is the complex local wave number in the intermediate state.

We then get the expression for the 2-step process cross section [7]

$$\left(\frac{\partial^2\sigma^{(2)}}{\partial\varepsilon_f\partial\Omega_f}\right) = \left(\frac{A}{A+1}\right)^4 \int \mathrm{d}E_m \int \mathrm{d}\mathbf{r}_1 \int \mathrm{d}\mathbf{r}_2 \frac{k_f/k_f(\mathbf{r}_2)}{k_i/k_i(\mathbf{r}_1)} \left|\chi_f^{(-)}(\mathbf{r}_2)\right|^2 \left|\chi_i^{(+)}(\mathbf{r}_1)\right|^2 \times \left(\frac{\partial^2\sigma}{\partial E_f\partial\Omega_2}\right)_{\mathbf{r}_2} \rho(\mathbf{r}_2) \frac{\exp(-2\gamma_m|\mathbf{r}_2 - \mathbf{r}_1|)}{|\mathbf{r}_2 - \mathbf{r}_1|^2} \left(\frac{\partial^2\sigma}{\partial E_m\partial\Omega_m}\right)_{\mathbf{r}_1} \rho(\mathbf{r}_1) \quad (13)$$

where $E_m(\mathbf{r}_1) = \hbar^2\kappa_m^2/2\mu$, and Ω_m is the direction of $\mathbf{r}_2 - \mathbf{r}_1$. The local average cross sections are given by (9) with appropriate substitutions of coordinates and momenta.

Eqs. (8) and (13) allow simple intuitive interpretations. Eq. (8) gives the cross section as an incoherent sum of local average cross sections at the individual points, $\mathbf{r}$, of the nucleus, each weighted by $|\chi_i(\mathbf{r})|^2|\chi_f(\mathbf{r})|^2$ which represents the probability of the incident particle reaching and the outgoing particle escaping from the collision point, $\mathbf{r}$. The fluxes of the fast particle are renormalized to the local values. Eqs. (13) can be interpreted in the same way as (8), plus the decrease in the flux of the fast particle in propagation from the first to the second collision points by the absorption of the potential and by the geometrical inverse square law. The interpretations described above are clearly consistent with the picture of INC. (8) and (13), however, take account of all the effects of the distorting potentials and of collisions in classically inaccessible regions of the nucleus which are not included in INC calculations.

Another interesting feature of (8) and (13) is that they predict, in agreement with observation, angular distributions without oscillatory patterns which are characteristic to direct reactions leading to discrete final states of the nucleus. The origin of such a pattern is the interference between outgoing waves generated at different points in the nucleus which are at a distance of the order of the nuclear dimension. In (8) and (13), such interference exists in the transition to the individual states, n, but is canceled out when the cross sections are summed over the n because of the random phases of the Φ_n, i.e. of the $\phi_\alpha\phi_\beta$, which make the range of K short and, consequently, the local collisions incoherent.

In fact, if Φ_n is a linear combination of $1p-1h$ states created on Φ_0 of the form of (2), K takes the form

$$K(\mathbf{r},\mathbf{r}') = \sum_n \sum_{\beta\alpha\beta'\alpha'} A_{\beta\alpha}^n A_{\beta'\alpha'}^{n*} \phi_\beta^*(\mathbf{r})\phi_\alpha(\mathbf{r})\phi_{\beta'}(\mathbf{r}')\phi_{\alpha'}^*(\mathbf{r}')\delta(\varepsilon_n - \varepsilon_0 - \omega) \quad (14)$$

where the $A_{\beta\alpha}^n$ are the coefficients of the linear combination. If the phases of the $A_{\beta\alpha}^n\phi_\beta^*(\mathbf{r})\phi_\alpha(\mathbf{r})$ are not random, but coherent for all $\beta\alpha$ and n, as in the case of excitation of a coherent state in the continuum such as a giant resonance, $K(\mathbf{r},\mathbf{r}')$ does not vanish even if $\mathbf{r}$ and $\mathbf{r}'$ are far apart, even at a distance of the order of nuclear dimension. The angular distribution then must show the diffraction like pattern, which is indeed observed in giant resonance excitations by (p,p') or (p,n).

In actual calculations, effective NN interaction in the nuclear medium must be used for v rather than the bare nuclear force, including spin and isospin dependence.

Exchange of the incident and the struck target protons must also be included. One can do it easily by modifying the r.h.s. of (2.10). If one uses experimental NN cross sections for $(\partial\sigma/\partial\Omega_{\kappa'})_{NN}$, the exchange effects are automatically included.

Another factor to be taken into account is the non-locality of the distorting potentials. The empirical local optical potentials we use for them should be considered to be the local equivalent potentials of the true, non-local optical potentials. We take account of this by means of the well known Perey factor [12]

$$F_c(r) = \left(1 - \frac{\mu b^2 U_c(r)}{2\hbar^2}\right)^{-1/2} \tag{15}$$

multiplying the wave functions of all the particles in the continuum where c = i, f, and β stand for the fast particle in the initial and the final states and a struck target nucleon in state β in the continuum respectively. The Perey factor is 1 for bound state wave functions in the Fermi gas model because of normalization. We multiply the Green function by $F_m(\mathbf{r}_1)$ and $F_m(\mathbf{r}_2)$ on either side of it.

Derivation of the cross section formulae for (p, nx) reactions is entirely analogous to $(p, p'x)$ reactions.

3. Results and discussions

The input data of numerical calculations are (a) the distorting potentials, (b) the in-medium NN scattering cross sections, and (c) the nuclear density distribution. For (a), we use the global nucleon optical potentials of Refs. [8] and [9]. For the calculation of the Perey factors, we use the range of non-locality $b = 0.85$fm. For (b), we use NN scattering cross sections in the nuclear medium given by Li and Machleit [10], and also those in the free space for comparison. For (c), we use $\rho(r) = \rho_0[1 + \exp((r-R)/a_0)]^{-1}$ where $R = r_0 A^{1/3}$ with $r_0 = (0.978 + 0.0206A^{1/2})$ fm and $a_0 = 0.54$ fm, ρ_0 is fixed by the normalization, $A = \int \rho(r)\mathrm{d}\mathbf{r}$ [11]

The 7-fold integration in the 2-step cross section is carried out by means of the method of quasi-random number Monte Carlo method [13]

The results of the calculations are shown in Figs. 1 through 4, and in Fig. 6. Figs. 1 and 2 show the angular distribution of $^{60}\mathrm{Ni}(p, p'x)$ at 200 MeV and 120 MeV respectively for the different outgoing proton energies, E'_p. Agreement with the experimental data is on the whole satisfactory. Agreement in the absolute magnitude of the cross sections is significant since the model has no adjustable parameter. The peak in the 1-step cross sections at high E'_p roughly corresponds to the quasi-elastic scattering. It is seen that the 2-step cross section is larger than the 1-step one at large and very small angles where the 1-step process is inhibited by the kinematics. The 2-step process gradually takes over the 1-step process as $E_{p'}$ gets lower.

Comparison with calculations with the three previous quantal models, FKK, TUL and NWY [5], is shown in Figs. 3 for the cases of $^{90}\mathrm{Zr}(p, p')$ at E_p =80 MeV and E'_p =40 MeV. In the three model calculations, a collective form factor is used whose strength is normalized in each model to fit the angle-integrated energy spectra at high E'_p. The SCDW cross section has no adjustable parameter. In all cases, the summed

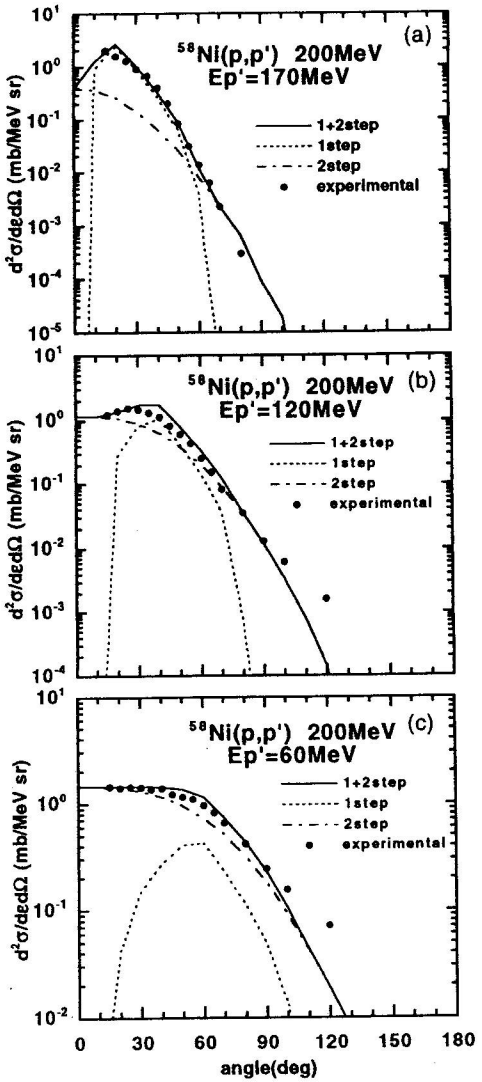

Fig. 1. SCDW double differential cross section for $^{60}\mathrm{Ni}(p, p'x)$ at E_p = 200 MeV and at E'_p = 170, 120 and 60 MeV. The dotted(dot-dashed) lines are 1(2)-step cross sections and the solid lines are the sum of the two. The closed circles are the data from Ref. [14].

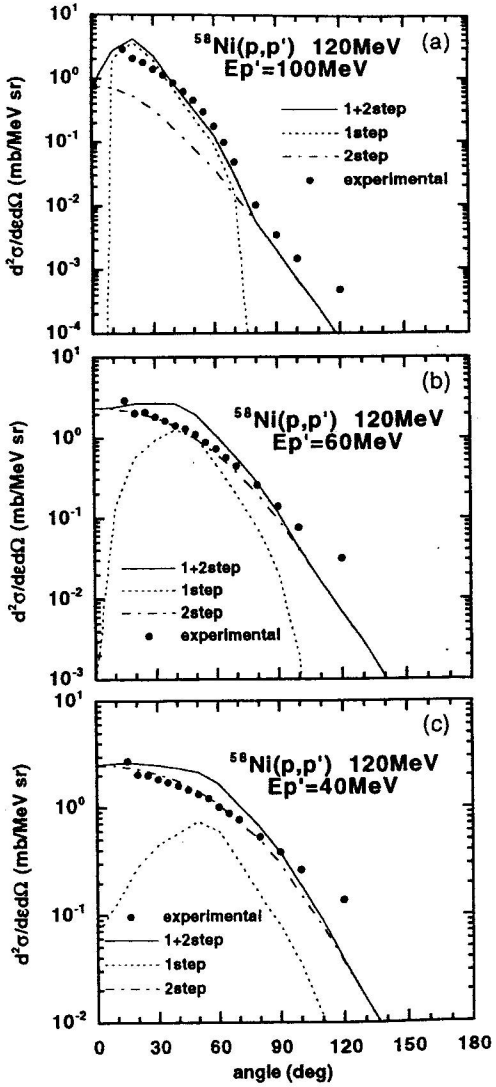

Fig. 2. The same as in Fig. 1 but at E_p = 120 MeV and E'_p = 100, 60 and 40 MeV.

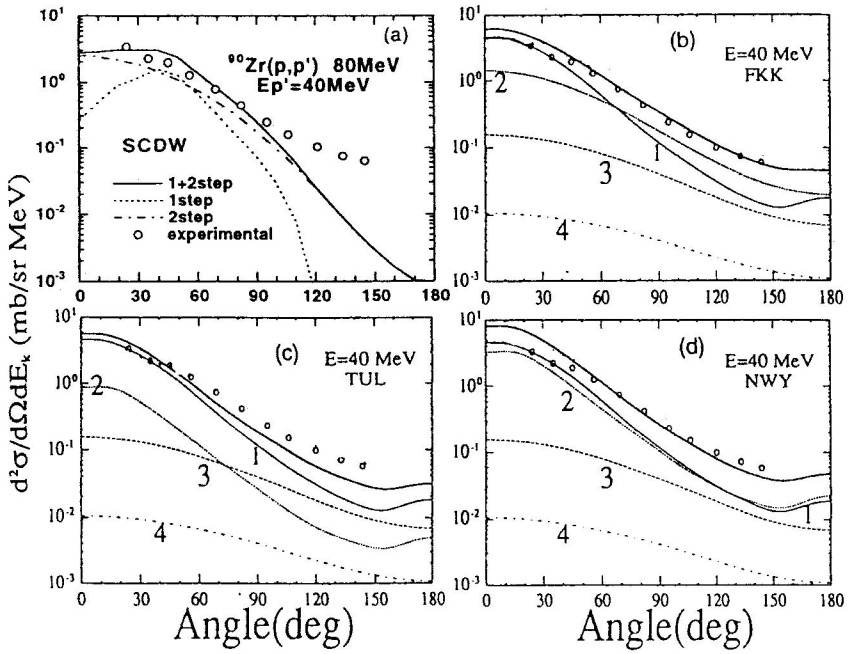

Fig. 3. Comparison of SCDW, FKK, TUL and NWY cross sections for ^{90}Zr$(p,p'x)$ at E_p =80 Mev and E'_p = 40 MeV. The notations for the SCDW cross sections are the same as in Fig. 1. For the other models, the lines with the numbers n are the n-step cross sections and the line without a number is the total sum.

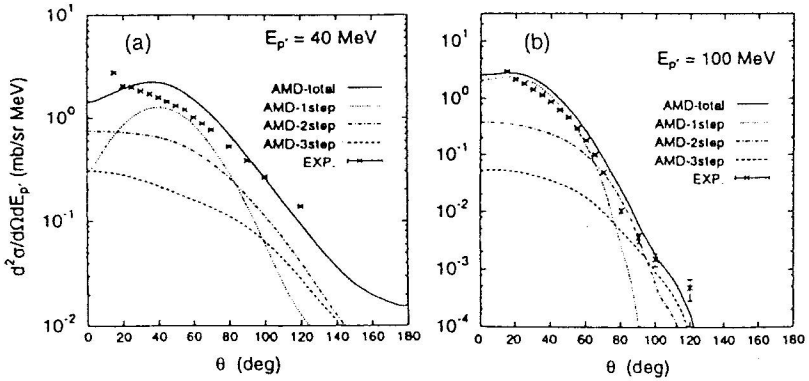

Fig. 4. AMD cross sections[3] and the data for the same cases as in Fig. 2. The dashed, dot-dashed and dotted lines are the 1- , 2- and 3-step cross sections respectively, and the solid line is the total sum. The crosses are the data taken from [15].

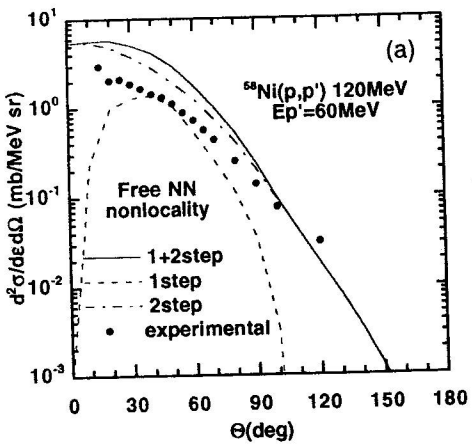

Fig. 5a. SCDW cross section for ^{60}Ni$(p,p'x)$ at E_p = 120 MeV and E'_p = 60 MeV with the NN cross sections in free space. The non-locality corrections are included.

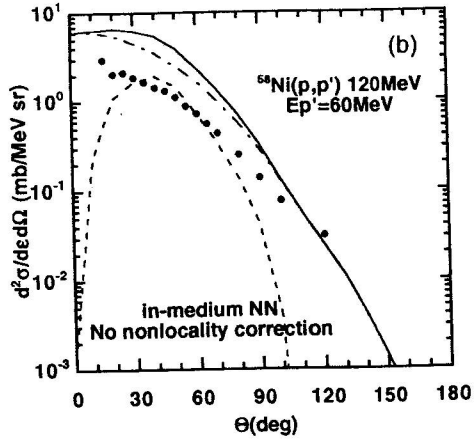

Fig. 5b. The same as in Fig. 5a but with the in-medium NN cross sections. The non-locality corrections are not included.

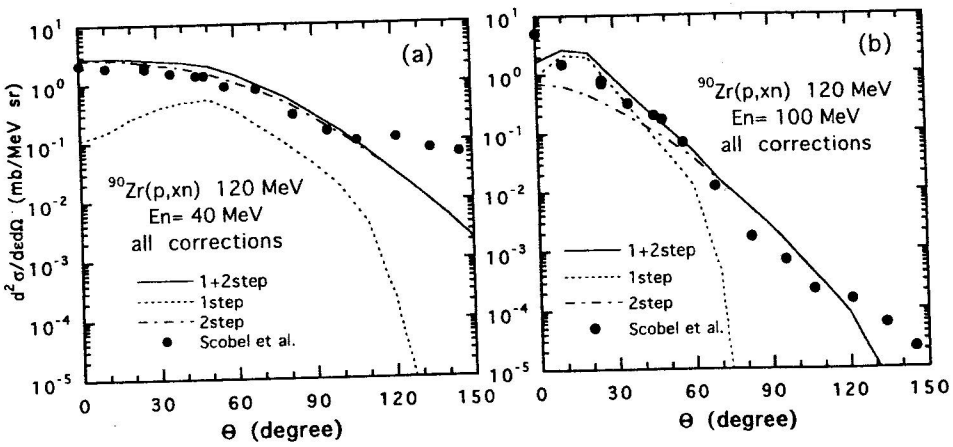

Fig. 6. SCDW cross sections for ^{90}Zr(p,nx) at E_p =120 MeV and E_n =100 MeV and 40 MeV. Notations are the same as in Fig. 1. The data from Ref. [16].

cross section of the 1- and 2-step processes agree with the data at angles less than 100°. The SCDW cross section then drops off the data, mainly because of the sharp

drop off of the 1-step cross section which is presumably due to small high momentum components in the degenerate Fermi gas model wave functions. Another possible reason for the underestimate at large angles is the effect of higher order processes, particularly 3-step process. The other models more or less maintain the agreement at large angles. Another noticeable difference between the SCDW and the other cross sections is that the 1-step cross section of SCDW has a peak at about quasi-elastic scattering angle while those of the other models do not. As a result, SCDW predicts predominance of the 2-step cross section over the 1-step one at forward angles in contrast to the other model. The reason for this is subject to further study. The 2-step cross sections of all the models disagree with each other. The SCDW cross section is, roughly, between the cross section of NWY and the ones of the other models.

The AMD cross sections of Ref. [3] are shown in Fig. 5 which should be compared with the SCDW cross sections in Fig. 2 for the same case of ^{60}Ni(p,p') at 120 MeV. Agreement is good in the cross section as a whole in every case. It is interesting to note that the AMD 1-step cross sections do show peaks at about the quasi-elastic scattering angle, though slightly shifted forward. This is in agreement with SCDW and in contrast to the 1-step cross sections of the three previous MSD models mentioned above. The 1-step cross section is predicted by AMD to be always dominant near the quasi-elastic peak, which is contrary to what is seen in Fig. 2.

One can see the effect of the medium correction to the NN interaction and that of the non-locality correction if one compares Fig. 2 with Figs. 5a and 5b which show the cross sections of ^{60}Ni$(p,p'x)$ at 120 MeV and E'_p =60 MeV calculated with the free-space NN cross section and with the non-locality correction and that with the in-medium NN cross section and without the non-locality correction respectively. One sees that the effects of the two kinds of corrections are roughly of the same order of magnitude and reduce the 2-step cross section much more strongly than the 1-step one. Together they bring the calculated cross section down close to the experimental data. The corrections are much smaller at $E'_p = 100$ MeV and much larger at $E'_p = 40$ MeV than at $E'_p = 60$ MeV, although they are not shown here,

Fig. 6 shows an example of (p, nx) reaction, for the case of ^{90}Zr(p,nx) at 120 MeV and E_n= 100 MeV and 40 MeV. Again, agreement with the experimental data is satisfactory, except at very large angles for the case of $E_n = 40$ MeV. The reason for the discrepancy is not clear for the moment. It could be due to higher order processes.

4. Summary

Semi-Classical Distorted Wave model (SCDW) for inclusive cross sections of multi-step direct processes in $(p,p'x)$ and (p,nx) reactions at intermediate energies is described, with explicit closed form expressions for the cross sections of 1- and 2-step direct processes. The expressions are consistent with the basic picture of intra nuclear cascade (INC) model that the cross section is a sum of the cross sections of successive local NN collisions with absorption in the propagation between consecutive collisions. SCDW, however, contains all the effects of the distorting potentials and the contribution of classically inaccessible region of the nucleus. It is shown that such a cross section is a result of the random phases of the final state nuclear wave functions which renders

the range of the kernel K of section 2 short. The same reason is responsible for the lack of diffraction-like oscillatory pattern in the angular distribution which is characteristic to direct reactions leading to discrete final states of the nucleus; the diffraction-like pattern in the angular distribution seen in the excitation of a giant resonance is due to the long range of K because of the coherent phases of the 1p1h components in the state.

Double differential cross sections of SCDW for $(p,p'x)$ on ^{60}Ni at 200 MeV and 120 MeV, and of (p,nx) on ^{90} Zr at 120 MeV agree well with experimental data on the whole, including the absolute magnitude. Use of the in-medium NN scattering cross sections and the correction due to the non-locality of distorting potentials are essential for the agreement. The effects of those corrections are larger on the 2-step than on the 1-step cross sections and at low than at high exit energies. Both corrections reduce cross sections. Extension of the model to higher energies, including meson degrees of freedom, will be very interesting.

Comparison of SCDW with the three previous quantal models, FKK, TUL and NWY with collective form factors [5] is made for the case of ^{90}Zr(p,p') at $E_p = 80$ MeV and $E'_p = 40$ MeV. All the 4 calculations agree with the data and with each other up to 100°. However, individual cross sections of the 1- and the 2-step processes do not agree with each other. Roughly, the SCDW 2-step cross section is between NWY and TUL ones. The drop off of the SCDW cross section at large angles is presumably due to the use of the degenerate Fermi gas model in SCDW. The behaviour of the 1-step cross section at forward angles is different in SCDW and the other models. It will be interesting to know which is likely to be the case in reality. SCDW agrees well with AMD for ^{60} Ni(p,p') at 120 MeV in the cross sections as a whole and in the shape of the 1-step cross sections, but not in the relative importance of 1- and 2-step processes: SCD W predicts dominance of the 2-step process at the lower exit energies while AMD predicts dominance of 1-step process at all exit energies near the qausi-elastic peak. It will be very interesting to see which prediction is better.

Extension of SCDW to 3-step processes is straight forward. It will be useful not only for analyses of experiments, but also for confirmation of the convergence of the model against increased number of steps. Application of SCDW to the cases of low exit energies will be more complicated since still higher order processes and compound nuclear processes are likely to be important there. In practice, connecting SCDW to some existing statistical models, such as Exciton model, may be more practical than straightforward continuation of higher order SCDW calculations. Whether that is feasible is a subject of future investigations.

Acknowledgements The authors wish to thank Drs. S. Chiba, T. Maruyama K. Niita, and to Drs. Horiuchi, A. Ono and E. I. Tanaka for their correspondences about their QMD and AMD calculations respectively and many stimulating discussions. They are much indebted to Professor Y. Akaishi for providing them with his computer code for Monte Carlo calculations and helpful advice. The financial aid of RCNP, Osaka University, for the computation is gratefully acknowledged. The work is partially supported by the Grant-in-Aid of the Japanese Ministry of Education, Science and Culture.

References

[1] *See, for example,* E. Gadioli, P.E. Hodgson: *Pre-Equilibrium Nuclear Reactions.* Oxford University Press, Oxford 1992

[2] S. Chiba, K. Niita, T. Maruyna *et al.*: *in Proc. 1994 Symp. on Nuclear Data, JAERI, Tokai 1994 (Eds. M. Kawai, T. Fukahori).* (JAERI-Conf 95008, 1995), p. 86;
S. Chiba, K. Niita, T. Maruyna *et al.*: *in Proc. 2nd Symp. on Simulation of Hadronic Many-Body System, JAERI, Tokai 1994 (Eds. A. Iwamoto, K. Niita, T. Maruyama).* (JAERI-Conf 95-012, 1995), p. 9

[3] E.I. Tanaka, A. Ono, A. Horiuchi, T. Maruyama, E. Engel: *Phys. Rev. C* **52** (1995) 316

[4] H. Feshbach, A.K. Kerman, S. Koonin: *Ann. of Phys.* **125** (1980) 429 *(hereafter referred to as FKK)*;
T. Tamura, T. Udagawa, H. Lenske: *Phys. Rev. C* **26** (1982) 379 *(hereafter referred to as TUL)*;
H. Nishioka, H.A. Weidenmüller, S. Yoshida: *Ann. of Phys.* **183** (1988) 166 *(hereafter referred to as NWY)*

[5] A.J. Koning, J.M. Akkermans: *Phys. Rev. C* **47** (1993) 724

[6] Y.L. Luo, M. Kawai: *Phys. Lett. B*, **235** (1990) 211;
Phys. Rev. C **43** (1991) 2367;
Y. Watanabe, M. Kawai: *Nucl. Phys.* **560** (1993) 43

[7] M. Kawai, H.A. Weidenmüller: *Phys. Rev. C* **45** (1992) 1856;
Y. Watababe: JAERI-Conf 96-012, 1995 (cited in ref. 3), p. 119 *(in Japanese)*

[8] R.L. Walter, P.P. Guss: *in Int. Nat. Conf. Nuclear Data Basis and Applied Science, Santa Fe 1985 (Ed. P.G. Young).* Gordon and Breach, New York 1986, p. 1075

[9] P. Schwandt *et al.*: *Phys. Rev. C* **26** (1982) 55

[10] G.Q. Li, R. Machleit: *Phys. Rev. C* **48** (1993) 1702

[11] J. W. Negele: *Phys. Rev. C* **1** (1970) 1260

[12] F.G. Perey, B. Buck: *Nucl. Phys.* **32** (1962) 353

[13] Y. Akaishi: *private communication (1993)*

[14] S.V. Förtsch, A.A. Cowley, J.J. Lawrie *et al.*: *Phys. Rev. C* **43** (1991) 691

[15] A.A. Cowley *et al.* : *Phys. Rev. C* **43** (1991) 678

[16] W. Scobel *et al.*: *Phys. Rev. C* **41** (1990) 2010.